Available online at www.sciencedirect.com
ScienceDirect
Biochimica et Biophysica Acta 1767 (2007) 114–123
Biochimica et Biophysica Acta
BBA
www.elsevier.com/locate/bbabio

# Structures of the $Ca^{2+}$–ATPase complexes with ATP, AMPPCP and AMPPNP. An FTIR study

Maria Krasteva, Andreas Barth *

*Department of Biochemistry and Biophysics, The Arrhenius Laboratories for Natural Sciences, Stockholm University, S-106 91 Stockholm, Sweden*

Received 30 August 2006; received in revised form 2 November 2006; accepted 7 November 2006
Available online 11 November 2006

**Abstract**

We studied binding of ATP and of the ATP analogs adenosine 5′-(β,γ-methylene)triphosphate (AMPCP) and β,γ-imidoadenosine 5′-triphosphate (AMPPNP) to the $Ca^{2+}$–ATPase of the sarcoplasmic reticulum membrane (SERCA1a) with time-resolved infrared spectroscopy. In our experiments, ATP reacted with ATPase which had AMPPCP or AMPPNP bound. These experiments monitored exchange of ATP analog by ATP and phosphorylation to the first phosphoenzyme intermediate $Ca_2$E1P. These reactions were triggered by the release of ATP from caged ATP. Only small differences in infrared absorption were observed between the ATP complex and the complexes with AMPPCP and AMPPNP indicating that overall the interactions between nucleotide and ATPase are similar and that all complexes adopt a closed conformation. The spectral differences between ATP and AMPPCP complex were more pronounced at high $Ca^{2+}$ concentration (10 mM). They are likely due to a different position of the γ-phosphate which affects the β-sheet in the P domain.


*Keywords:* Infrared spectroscopy; $Ca^{2+}$ pump; SERCA1a; Caged ATP; ATP binding; Nucleotide binding

## 1. Introduction

$Ca^{2+}$–ATPases [1] and related P-type ATPases are multi-domain proteins that couple uphill ion transport to ATP hydrolysis via molecular movement within and between domains. A prominent example is the sarcoplasmic reticulum $Ca^{2+}$–ATPase which mediates muscle relaxation by the removal of cytosolic $Ca^{2+}$. Key events for $Ca^{2+}$–ATPase function are $Ca^{2+}$, $H^+$ and ATP binding, as well as phosphorylation of D351 by ATP and the interconversion between two phosphoenzyme intermediates, $Ca_2$E1P and E2P.

Binding of two cytosolic $Ca^{2+}$ (E2/E1 → $Ca_2$E1) enables ATP to phosphorylate D351 of the ATPase which occludes the bound $Ca^{2+}$. The first phosphoenzyme intermediate ($Ca_2$E1P), which is ADP-sensitive, converts to an ADP-insensitive form (E2P) that is more rapidly hydrolysed. Phosphoenzyme conversion is associated with $Ca^{2+}$ release towards the sarcoplasmic reticulum lumen against the concentration gradient. E2P picks up protons from the lumenal side of the membrane that are counter-transported and released to the cytoplasmic side upon $Ca^{2+}$ binding [2–4].

Binding of ATP induces conformational changes that are relatively large compared to those associated with the phosphorylation reaction as seen by infrared spectroscopy [5]. The conformational change upon nucleotide binding depends to a surprising degree on individual interactions between ATPase and nucleotide [6,7]. It was concluded that the ATPase interacts with the γ-phosphate [7], the ribose hydroxyls and the amino function [6] of ATP. The missing of individual interactions produces more than just local effects: it affects the entire conformational change upon binding. This suggests a concerted conformational change for which all interactions need to be in place [6]. TNP-AMP binding to $Ca_2$E1 seems to cause small structural changes that are largely

*Abbreviations:* AMPCP, adenosine 5'-(β,γ-methylene)triphosphate; AMPPNP, β,γ-imidoadenosine 5'-triphosphate; AMPPXP, AMPPCP or AMPPNP; $Ca_2$E1, $Ca^{2+}$ bound form of $Ca^{2+}$–ATPase; $Ca_2$E1P, ADP-sensitive phosphoenzyme; caged ATP, $P^3$-1-(2-nitrophenyl)ethyl ATP; caged AMPPNP, $P^3$-1-(2-nitrophenyl)ethyl AMPPNP; E2P, ADP-insensitive phosphoenzyme; FTIR, Fourier transform infrared

* Corresponding author. Tel.: +46 8 162452; fax: +46 8 155597.
*E-mail address:* Andreas.Barth@dbb.su.se (A. Barth).

0005-2728/$ - see front matter © 2006 Elsevier B.V. All rights reserved.
doi:10.1016/j.bbabio.2006.11.003

opposite to those induced by ATP [8]. As a consequence, the (average) structure of the nucleotide–ATPase complex is characteristic of the nucleotide bound. This explains some of the conflicting results obtained with different ATP analogs for the $Ca^{2+}$–ATPase and the $Na^{+}/K^{+}$–ATPase which has led to a controversy about the number of binding sites as summarised previously [9,10].

The interactions identified by infrared spectroscopy were later confirmed by X-ray crystallography [11,12]. Binding of ATP closes a cleft between two of the cytoplasmic domains of the ATPase [13,14]: the nucleotide-binding domain (N domain) and the phosphorylation domain (P domain). Closure of the cleft delivers the γ-phosphate to the phosphorylation site D351 in the P domain [11,12]. The two domains are bridged by ATP in the ATP–ATPase complex ($Ca_2$E1ATP) which also provides an explanation for the drastic structural effects of modifying the ribose 3′-OH and the adenine amino function. Interactions of both groups stabilize the closed conformation of the complex, 3′-OH directly via an interaction with R678 in the P domain, the amino group indirectly because its interaction with K515 seems to position the ribose hydroxyls such that interaction with the P domain is possible.

The X-ray structures of the ATP bound state $Ca_2$E1ATP [11,12] were obtained with the ATP analog AMPPCP instead of ATP. These structures are almost identical to the structures of a $Ca_2$E1P analog [12,15]. In particular, in both states the side chain orientation of the $Ca^{2+}$ ligand E309 is locked [11] and a putative $Ca^{2+}$ access channel between transmembrane helices M1 and M2 is closed off [12]. This similarity between the two structures obscures the structural cause for the functional difference between the ATP bound state and $Ca_2$E1P. In the ATP bound state the $Ca^{2+}$ ions are accessible whereas they are occluded in $Ca_2$E1P. A recent study has shed light on this paradox concluding that the $Ca_2$E1AMPPCP complex has different properties and structures at μM and mM $Ca^{2+}$ concentration and resembles at low $Ca^{2+}$ concentration more the ATP complex and at high $Ca^{2+}$ concentration more $Ca_2$E1P [16]. In particular, $Ca^{2+}$ dissociation is slowed down by AMPPCP at high but not at low $Ca^{2+}$ concentrations. High $Ca^{2+}$ concentration have been used to obtain the crystal structure of the AMPPCP complex [11] whereas most other studies have been done at lower $Ca^{2+}$ concentration.

Here we investigate with infrared spectroscopy the structures of the $Ca^{2+}$–ATPase complexes with ATP, AMPPCP and AMPPNP (see Fig. 1 for the structures of these nucleotides). We show that the structures of the complexes with AMPPNP and AMPPCP are similar to each other as seen by infrared spectroscopy but that they are slightly different from that of the complex with ATP.

We use the photolytic release of effector molecules from inactive, photosensitive precursors (caged compounds) to start the partial reactions of the $Ca^{2+}$–ATPase [17–19]. This allows the sensitive detection of the small infrared absorbance changes that are associated with these reactions. These changes reflect changes of protein structure in the amide I and amide II region of the infrared spectrum and environmental changes like changes in hydrogen bonding. The sensitivity is high enough to detect environmental changes around single atoms in this 15000 atom protein [20].

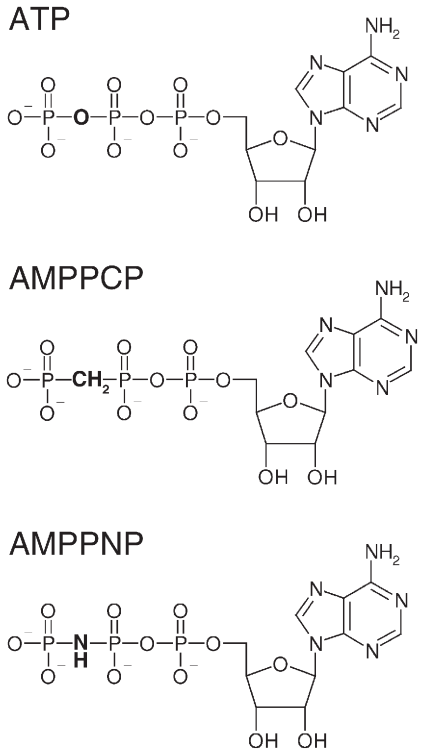


Fig. 1. Structures of ATP, AMPPCP and AMPPNP. The differences between these structures are shown in bold.

## 2. Materials and methods

### 2.1. Sample preparation

Samples for infrared spectroscopy were prepared as described [21]. SR vesicles were dialysed in the presence of 15 μM $Ca^{2+}$ which saturates the $Ca^{2+}$ binding sites of the ATPase. A vesicle suspension together with additions was then dried on a $CaF_2$ window and subsequently rehydrated with water. Approximate concentrations in $Ca^{2+}$ samples were: 100–150 mg/ml protein, 300 mM Mops/KOH pH 7.0, 150 mM KCl, 10 mM free $CaCl_2$, 20 mM glutathione, 50 mM AMPPNP or AMPPCP, 12 or 20 mM caged ATP, 0.5 mg/ml $Ca^{2+}$ ionophore A23187, and 1–2 mg/ml adenylate kinase. Low $Ca^{2+}$/high $Mg^{2+}$ samples contained 3 mM $MgCl_2$ and 0.15 mM free $CaCl_2$ (i.e. not counting the $Ca^{2+}$ bound to the ATPase which corresponded to ~2 mM) instead of 10 mM $CaCl_2$. Control samples contained 200 mM instead of 50 mM AMPPCP. This is expected to slow down nucleotide exchange and subsequent protein reactions considerably. Accordingly, no bands of ATPase phosphorylation can be seen in these spectra indicating that phosphoenzyme decay is no longer rate-limiting. Samples in $^{2}H_2O$ were prepared in the same way as $^{1}H_2O$ samples but rehydrated with $^{2}H_2O$. The protein concentration in our samples might be perceived as high but is slightly less than found in cells [22]. In addition, the ATPase concentration within the sarcoplasmic reticulum membrane is not altered by our sample preparation.

### 2.2. FTIR measurements

Time-resolved FTIR measurements were performed at 1 °C as described [5,23]. Several experiments were averaged and the spectra normalized to equal protein content as described [23]. Binding of AMPPCP and AMPPNP were studied in displacement experiments. The initial state in these experiments was $Ca_2$E1AMPPXP where AMPPXP stands for AMPPNP or AMPPCP. Displacement of AMPPXP by ATP and subsequent transition to $Ca_2$E1P was triggered by

the release of ATP from caged ATP. The sample composition was such that $Ca_2E1P$ accumulated and its decay was rate limiting. To study nucleotide binding in displacement experiments may seem complicated, but is a direct way to assess structural differences between two nucleotides. The small absorbance differences between two nucleotides can be recorded with very high fidelity because they are obtained in single time-resolved experiments. This avoids comparison of spectra obtained with different samples which might give rise to artifacts. Because of similar results with AMPPCP and AMPPNP, only the AMPPCP spectra are shown and their experimental details described. For AMPPCP, the displacement experiments yielded spectra of the complete reaction to the first phosphoenzyme intermediate $Ca_2E1AMPPCP \rightarrow Ca_2E1P$ and of the partial reactions of (i) nucleotide exchange $Ca_2E1AMPPCP \rightarrow Ca_2E1ATP$ and (ii) of phosphorylation after exchange of AMPPCP for ATP $Ca_2E1ATP \rightarrow Ca_2E1P$.

The *AMPPCP→E1P spectrum* reflects the absorbance change that is associated with the reaction $Ca_2E1AMPPCP \rightarrow Ca_2E1P$. It is the absorbance of $Ca_2E1P$ minus that of $Ca_2E1AMPPCP$. The absorbance change with respect to a spectrum before ATP release was recorded 14–68 s after ATP release for $Ca^{2+}/{}^1H_2O$ samples, 12–31 s after ATP release for $Ca^{2+}/{}^2H_2O$ and $Mg^{2+}/{}^1H_2O$ samples and 12–20 s after ATP release for $Mg^{2+}/{}^2H_2O$ samples.

The *nucleotide exchange spectrum* was obtained in the early phase of a displacement experiment. It reflects the absorbance change associated with exchange of AMPPCP by ATP on the ATPase: $Ca_2E1AMPPCP \rightarrow Ca_2E1ATP$. It is the absorbance change 0.14–1.2 s after ATP release for $Ca^{2+}/{}^1H_2O$ samples, and that 0.14–0.68 s after ATP release for $Ca^{2+}/{}^2H_2O$, $Mg^{2+}/{}^1H_2O$ and $Mg^{2+}/{}^2H_2O$ samples.

The *phosphorylation spectrum in the presence of AMPPCP* was obtained in the later phase of a displacement experiment $Ca_2E1AMPPCP \rightarrow Ca_2E1ATP \rightarrow Ca_2E1P$ and predominantly reflects the change in absorbance between $Ca_2E1ATP$ and $Ca_2E1P$ (absorbance of $Ca_2E1P$ minus that of $Ca_2E1ATP$). Therefore it is expected to have the same shape as the phosphorylation spectrum in the absence of AMPPCP [5,23] which reflects the same reaction. The phosphorylation spectrum in the presence of AMPPCP was calculated for $Ca^{2+}/{}^1H_2O$ samples by subtraction of spectra obtained 0.14–3.2 s and 14–68 s after ATP release. The time interval for the early spectrum characterising $Ca_2E1ATP$ was extended with respect to that used to characterise the same state in the nucleotide exchange spectrum in order to achieve a better signal to noise ratio. Modifying the time interval for the early spectrum in the subtraction did not change the shape of the resulting spectrum.

From the time constant for the rise of the marker band of the phosphorylation reaction at 1719 $cm^{-1}$ [5,24,25] it was calculated that at the time of recording the 0.14–3.2 s spectrum already 34% of the ATPase molecules were phosphorylated in the $Ca^{2+}/{}^1H_2O$ samples. Thus the spectrum resulting from the subtraction represents only 66% of the full extent of the phosphorylation reaction. Therefore it was multiplied by 1.52 (=100%/66%) and the resulting spectrum is termed phosphorylation spectrum in the presence of AMPPCP.

## 3. Results

### 3.1. AMPPCP→ATP displacement experiments at high $Ca^{2+}$

Binding of AMPPCP and AMPPNP to the $Ca^{2+}$–ATPase was studied in displacement experiments. The initial state in these experiments was therefore $Ca_2E1AMPPCP$ or $Ca_2E1AMPPNP$. Release of ATP from caged ATP triggered exchange of AMPPXP by ATP and subsequent phosphorylation to $Ca_2E1P$. Only experiments with AMPPCP are shown, since the results with AMPPNP were similar. For experiments with AMPPCP under different conditions, Fig. 2A–C show spectra of the full reaction $Ca_2E1AMPPCP \rightarrow Ca_2E1P$ as thin lines (AMPPCP→E1P spectra) and of the first partial reaction,

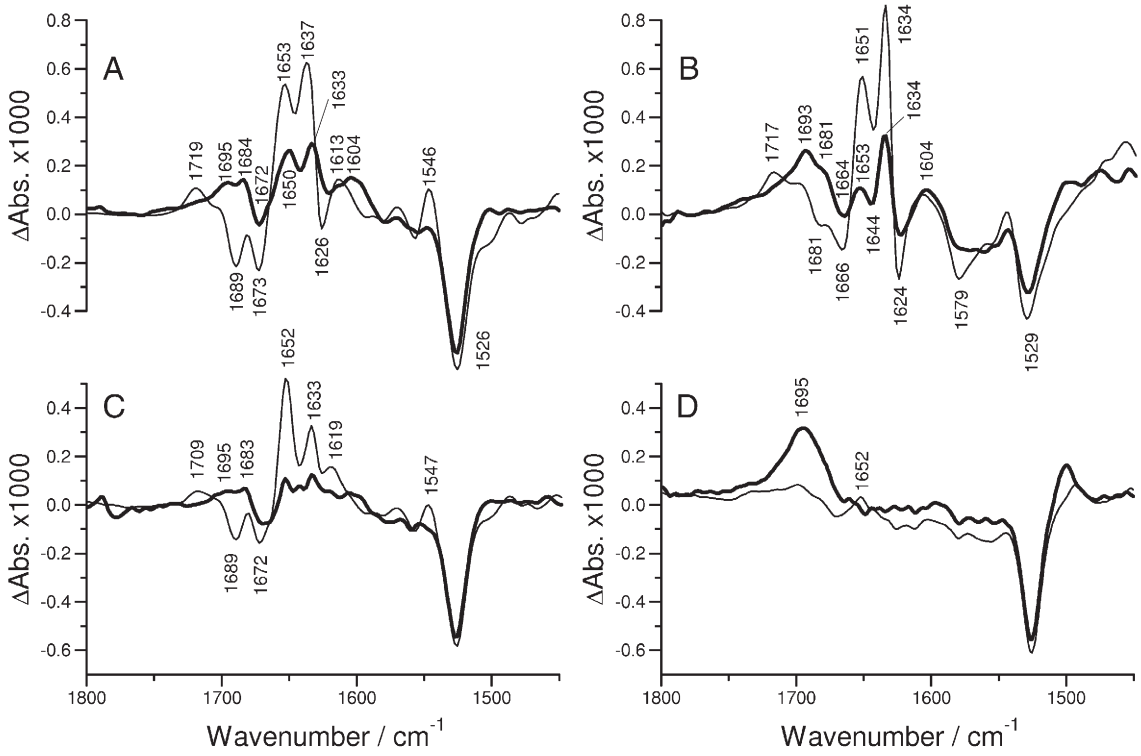


Fig. 2. Infrared difference spectra of displacement experiments in which AMPPCP was replaced by ATP at pH 7, 1 °C. The initial state in these experiments was $Ca_2E1AMPPCP$. The transition to $Ca_2E1P$ was triggered by the release of ATP from caged ATP. (A)–(C) Bold line: nucleotide exchange spectrum reflecting $Ca_2E1AMPPCP \rightarrow Ca_2E1ATP$. Thin line: AMPPCP→E1P spectrum in ${}^1H_2O$ reflecting $Ca_2E1AMPPCP \rightarrow Ca_2E1P$. (A) 10 mM $Ca^{2+}$ in ${}^1H_2O$. (B) 10 mM $Ca^{2+}$ in ${}^2H_2O$. (C) 0.15 mM $Ca^{2+}$ and 3 mM $Mg^{2+}$ in ${}^1H_2O$. (D) Control spectra obtained with samples that contained 200 mM instead of 50 mM AMPPCP recorded 0.14–1.2 s (bold line) and 14.4–72 s (thin line) after ATP release. These times of spectra recording were the same as for the spectra in (A).

nucleotide exchange $Ca_2E1AMPPCP \rightarrow Ca_2E1ATP$, as bold lines (nucleotide exchange spectra). Fig. 3 shows the second partial reaction as bold line: phosphorylation after exchange of AMPPCP for ATP $Ca_2E1ATP \rightarrow Ca_2E1P$ (phosphorylation spectrum in the presence of AMPPCP). For comparison, the respective spectrum in the absence of AMPPCP is also shown as dotted line in Fig. 3. Fig. 2D shows control spectra recorded at the same times as the spectra in Fig. 2A.

The spectral range shown covers the amide I (1700–1610 $cm^{-1}$) and amide II (1580–1520 $cm^{-1}$) regions of the infrared spectrum which are both sensitive to structural changes of the peptide backbone. The main focus of the discussion is on the amide I region. Amino acid side chains can contribute in the whole spectral region shown. The large band near 1526 $cm^{-1}$ is mainly due to the photolysis of caged ATP [18,26,27].

Fig. 2A shows spectra obtained at different times in a displacement experiment at 10 mM $Ca^{2+}$ in $^1H_2O$. After ATP release, the ATPase became phosphorylated as indicated by the marker band for phosphorylation at 1719 $cm^{-1}$ [5,24,25] in the AMPPCP → E1P spectrum (thin line in Fig. 2A). A control spectrum recorded in the same time interval is shown as thin line in Fig. 2D. It shows only very small bands, and its subtraction from the AMPPCP → E1P spectrum (not shown) produced only small changes in the amide I region. It was interesting to observe that the negative 1673 $cm^{-1}$ band developed faster than most of the other bands, in particular than the band at 1719 $cm^{-1}$. An early stage of the reaction from $Ca_2E1AMPPCP$ to $Ca_2E1P$ is shown as bold line in Fig. 2A which is attributed predominantly to the exchange of AMPPCP by ATP, i.e. it shows the absorbance of $Ca_2E1ATP$ minus that of $Ca_2E1AMPPCP$. Apart from the band at 1672 $cm^{-1}$, this spectrum exhibits additional bands in the amide I region: the positive bands at 1650 and 1633 $cm^{-1}$. The three bands indicate differences between the structures of the ATP and AMPPCP complexes. None of the bands at 1672, 1650 and 1633 $cm^{-1}$ in the nucleotide exchange spectrum is seen in the control spectrum recorded in the same time interval (bold line in Fig. 2D) at 4-fold higher AMPPCP concentration. Accordingly, a subtraction of the control spectrum does not eliminate these bands (not shown). However, the control spectrum shows a positive band at 1695 $cm^{-1}$ because of which we do not interpret the positive bands at 1695 and 1684 $cm^{-1}$ in the nucleotide exchange spectrum. The 1695 $cm^{-1}$ band in the early control spectrum and the 1652 $cm^{-1}$ band in the later spectrum are associated with photolysis byproducts [18,27].

Fig. 2B shows spectra in $^2H_2O$ which correspond to the $^1H_2O$ spectra shown in panel a. Slightly different time intervals were used for the spectra in $^2H_2O$. Similar band profiles and peak positions are observed in $^1H_2O$ and $^2H_2O$. The band at 1672 $cm^{-1}$ is slightly downshifted to 1664 $cm^{-1}$ which is indicative of amide I bands. The best assignment of this band is to turn structures because the band positions in $^1H_2O$ and $^2H_2O$ are both outside the range usually given for the high wavenumber component of β-sheets [28,29]. The bands at 1650 and 1633 $cm^{-1}$ shift slightly towards higher wavenumbers. Several explanations for this are possible. (i) Part of the 1650 $cm^{-1}$ band in $^1H_2O$ seems to shift down, leaving a smaller band at 1653 $cm^{-1}$ in $^2H_2O$ and increasing the intensity on the high wavenumber side of the 1633 $cm^{-1}$ band ($^1H_2O$ band position). As a consequence, the band position is shifted up to 1634 $cm^{-1}$ in $^2H_2O$. Shifts and changes in absorption coefficient of other overlapping bands could further contribute to an apparent upshift of the 1633 $cm^{-1}$ band. (ii) Amide I bands could be overlapped differently in $^1H_2O$ and $^2H_2O$ by other, unidentified bands of side chains. (iii) The bands might originate from absorbance changes of carboxylate groups of a Glu or Asp residue. The band of the antisymmetric stretching vibration of carboxylate groups exhibits an upshift of 9 $cm^{-1}$ in $^2H_2O$ for groups that are completely exposed to water [30,31]. A carboxylate band at 1633 or 1650 $cm^{-1}$ would indicate that this carboxylate group chelates a metal ion in the bridging or unidentate mode [31–33].

Particular in the case of the 1633 $cm^{-1}$ band, we think that the observed upshift most likely is an apparent one because of overlap by negative bands on both sides of the 1633 $cm^{-1}$ band. This overlap is different in $^1H_2O$ and $^2H_2O$: on the low wavenumber side a negative band at 1624 $cm^{-1}$ is observed clearly only in $^2H_2O$ and on the high wavenumber side the negative band at 1642 $cm^{-1}$ in $^1H_2O$ (not labeled in Fig. 2A) is found at 1644 $cm^{-1}$ in $^2H_2O$. The combined effect of the negative bands and the partial downshift of the 1650 $cm^{-1}$ band will shift the 1633 $cm^{-1}$ band up in $^2H_2O$. In conclusion, we tentatively assign the 1633 $cm^{-1}$ band to an amide I vibration of a β-sheet because its band position seems to be essentially unchanged in $^2H_2O$. This indicates that the involved backbone section does not undergo $^1H/^2H$ exchange and thus is rather rigid. The alternative assignment to a polar or charged side chain that is insensitive to solvent deuteration is less likely since polar side chains usually exchange much faster than amide protons [34] in line with experiments showing exchange within several minutes [35,36].

Bands near 1630 $cm^{-1}$ are indicative of β-sheets with a considerable number of parallel or antiparallel strands and we have previously tentatively assigned the large bands at 1641 and 1627 $cm^{-1}$ in nucleotide binding spectra to the structural change of the β-sheet in the P domain [37]. Thus it is tempting to speculate that the 1633 $cm^{-1}$ band in the nucleotide exchange spectrum (bold line in Fig. 2A) is also caused by amide I vibrations of the β-sheet in the P domain. This β-sheet is better aligned in the ATP bound structure [11]. The better the alignment, the more strands participate in the coupled amide I vibrations of the β-sheet, and the lower will be the band position [38,39]. The band position at 1633 $cm^{-1}$ would then indicate involvement of parts of the β-sheet that are less well aligned than those corresponding to the main band at 1627 $cm^{-1}$ in ATP and AMPPNP binding spectra [5,40]. In the nucleotide exchange spectrum in $^2H_2O$ (bold line in Fig. 2B) the positive bands in the β-sheet region is accompanied by a negative band at 1624 $cm^{-1}$. This could indicate a shift of a small portion of the main band towards higher wavenumbers, implying that parts of the β-sheet become less well aligned upon AMPPCP → ATP exchange.

A kinetic evaluation (not shown) of the band at 1719 in $^1H_2O$ and of that at 1717 $cm^{-1}$ in $^2H_2O$ gives rate constants for

phosphorylation of 0.25 $s^{-1}$ (time constant 4 s) in $^1H_2O$ and of 0.3 $s^{-1}$ (time constant 3.5 s) in $^2H_2O$. These rates are 3-fold slower than those of phosphorylation in the absence of AMPPCP [5]. The rates in the presence of AMPPCP suggest that at the time of recording of the nucleotide exchange spectra in Fig. 2A and B, about 15% of $Ca_2$E1P had already formed in $^1H_2O$ and 11% in $^2H_2O$. However, a correction (not shown) of this contribution by subtraction of the phosphorylation spectrum in the presence of AMPPCP (see Fig. 3) produced only slightly altered nucleotide exchange spectra. A notable difference in $^1H_2O$ was a slight shift of the 1633 $cm^{-1}$ band to 1631 $cm^{-1}$ caused by subtraction of the 1638 $cm^{-1}$ phosphorylation band. Also in an nucleotide exchange spectrum recorded in the shorter time interval of 0.14–0.64 s, the band is found at 1631 $cm^{-1}$.

### 3.2. AMPPCP→ATP displacement experiments at low $Ca^{2+}$ and high $Mg^{2+}$

Fig. 2C shows spectra of experiments with 0.15 mM free $Ca^{2+}$ and 3 mM $Mg^{2+}$ instead of 10 mM $Ca^{2+}$ in $^1H_2O$. The $Ca^{2+}$ binding sites of the ATPase were saturated because the $Ca^{2+}$ concentration was never lower than 15 μM during sample preparation. The experiments were done to investigate whether the differences between AMPPCP and ATP binding are specific for $Ca^{2+}$ as might be expected from the previous studies [16]. The nucleotide exchange spectrum shows a broad negative band at 1669 $cm^{-1}$ (not labeled in Fig. 2C). Otherwise the spectrum is nearly featureless in the amide I region: only very small bands are observed at 1652 and 1633 $cm^{-1}$. At the time of recording the nucleotide exchange spectrum, the ATPase was phosphorylated to 18%. Correction of this contribution by subtracting the phosphorylation spectrum in the presence of AMPPCP did not significantly change the spectrum, it enhanced somewhat the 1683/1669 $cm^{-1}$ difference feature and reduced the small 1652 $cm^{-1}$ band, but not the 1633 $cm^{-1}$ band. The AMPPCP→E1P spectrum at low $Ca^{2+}$/high $Mg^{2+}$ bears strong resemblance to the AMPPNP→E1P spectrum at high $Ca^{2+}$ (not shown) and is also similar to the AMPPCP→E1P spectrum shown in Fig. 2A.

High $Ca^{2+}$ and low $Ca^{2+}$/high $Mg^{2+}$ conditions produce both the negative band near 1670 $cm^{-1}$ in nucleotide exchange spectra (compare bold lines in Fig. 2A and C). Under low $Ca^{2+}$/high $Mg^{2+}$ conditions the band seems to be broader than at high $Ca^{2+}$. This causes the shoulder on the low wavenumber side of the 1672 $cm^{-1}$ band in the AMPPCP→E1P spectrum (thin line in Fig. 2C) which is not observed with high $Ca^{2+}$ (thin line in Fig. 2A). The 1650 and 1633 $cm^{-1}$ bands of the nucleotide exchange spectrum with high $Ca^{2+}$ (bold line spectrum in Fig. 2A) are only just observed at low $Ca^{2+}$ in the presence of $Mg^{2+}$ (bold line spectrum in Fig. 2C). For the 1633 $cm^{-1}$ band, this is in line with the relatively reduced amplitude of this band in the AMPPCP→E1P spectrum at low $Ca^{2+}$/high $Mg^{2+}$ (compare thin line spectra in Fig. 2A and C). The much reduced bands at 1650 and 1633 $cm^{-1}$ indicate less structural changes upon AMPPCP→ATP exchange at low $Ca^{2+}$/high $Mg^{2+}$ as compared to high $Ca^{2+}$. This implies that the structure of the AMPPCP complex is more like that of the ATP complex under low $Ca^{2+}$/high $Mg^{2+}$ conditions.

In the AMPPCP→E1P spectra in $^1H_2O$ there is a small shift of the highest wavenumber band from 1719 $cm^{-1}$ in the presence of $Ca^{2+}$ (thin line in Fig. 2A) to 1718 $cm^{-1}$ with $Mg^{2+}$ (thin line in Fig. 2C). This has been observed before in the absence of AMPPCP [24,25] and supports the assignment of this band to the C=O group of phosphorylated D351. Similarly in $^2H_2O$, the band is found at 1717 $cm^{-1}$ with $Ca^{2+}$ (Fig. 2B) and at 1709 $cm^{-1}$ with $Mg^{2+}$ (not shown).

### 3.3. Phosphorylation spectra at high $Ca^{2+}$

After AMPPCP is exchanged by ATP, the phosphorylation reaction ($Ca_2$E1ATP→$Ca_2$E1P) is expected to be the same as in experiments where ATP is released in the absence of AMPPCP. This is scrutinized in Fig. 3 where the phosphorylation spectrum in the absence of AMPPCP (dotted line) is compared to that in its presence (bold line). In the amide I spectral region between 1610 and 1700 $cm^{-1}$, bands are found at the same positions and with the same sign. Even the amplitudes agree very well if it is considered that both spectra were normalized as described in Materials and methods. The small difference between the spectra resembles a spectrum of AMPCP→ATP exchange with bands at 1673 and 1637 $cm^{-1}$ which seem to indicate that AMPPCP→ATP exchange is still ongoing during the time interval that was used to record the phosphorylation spectrum in the presence of AMPPCP. Indeed, the amplitude of the 1673 $cm^{-1}$ band is larger in the AMPPCP→E1P spectrum (thin line in Fig. 2A) than in the nucleotide exchange spectrum (bold line in Fig. 2A) indicating that exchange is not complete at the time of recording the exchange spectrum. Upon correcting

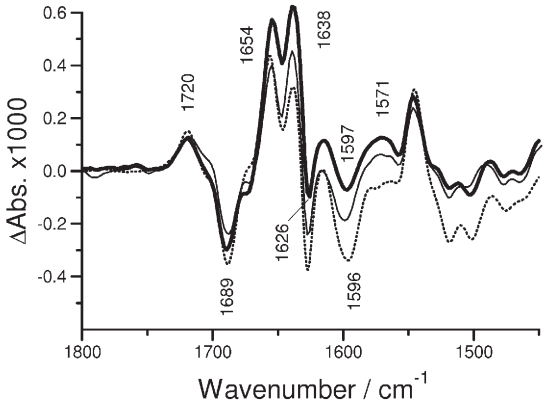


Fig. 3. Comparison of phosphorylation spectra in the presence and absence of AMPPCP in $^1H_2O$. Both spectra reflect predominantly $Ca_2$E1ATP→$Ca_2$E1P. Bold line: spectrum obtained in the later phase of a displacement experiment: $Ca_2$E1AMPPCP→$Ca_2$E1ATP→$Ca_2$E1P. Dotted line: spectrum obtained in the later phase of experiments in the absence of AMPPCP: $Ca_2$E1→$Ca_2$E1ATP→$Ca_2$E1P [5,23]. Thin line: phosphorylation spectrum in the presence of AMPPCP corrected for ongoing nucleotide exchange. First, the control spectrum (bold line in Fig. 2D) was subtracted from the nucleotide exchange spectrum (bold line in Fig. 2A). This eliminates signals from the photolysis of caged ATP in the nucleotide exchange spectrum. The resulting spectrum was multiplied by 0.6 and subtracted from the phosphorylation spectrum in the presence of AMPPCP.

the phosphorylation spectrum in the presence of AMPPCP for the contribution of ongoing nucleotide exchange, we obtained the thin line spectrum of Fig. 3. The agreement of this spectrum with the phosphorylation spectrum in the absence of AMPPCP is even better, in particular the relative amplitudes of the negative bands. This indicates that the structural changes upon phosphorylation are the same in the presence and absence of AMPPCP.

Correction of the nucleotide exchange spectrum for the full extent of nucleotide exchange makes it comparable in amplitude to the phosphorylation spectrum, indicating a similar extent of net backbone structural change. As discussed for the 1633 $cm^{-1}$ band in the nucleotide exchange spectrum, the 1638 $cm^{-1}$ band in the phosphorylation spectrum (dotted line in Fig. 3) could be caused by a part of the β-sheet in the P domain that becomes less well aligned upon phosphorylation.

### 3.4. Experiments with AMPPNP at high $Ca^{2+}$

With AMPPNP, the AMPPNP → E1P spectrum (not shown) was similar to the respective spectrum with AMPPCP with bands at 1722 (+), 1701 (+), 1690 (−), 1673 (−), 1653 (+) and 1634 (+) $cm^{-1}$. In addition, a subtraction of an AMPPNP binding spectrum from an ATP binding spectrum (not shown) produced a spectrum similar to the nucleotide exchange spectrum with AMPPCP (bold line in Fig. 2A) with bands at 1696 (+), 1686 (+), 1671 (−), 1661 (+) and 1632 $cm^{-1}$ (+). With AMPPNP it was less obvious than with AMPPCP that the 1672/1673 $cm^{-1}$ band develops faster than the marker band for phosphorylation at 1719 $cm^{-1}$. This can be attributed to the nucleotide exchange reaction and the subsequent phosphorylation reaction being more convoluted because exchange is nearly rate limiting in these experiments. Otherwise, AMPPNP behaved similar to AMPPCP in our experiments.

## 4. Discussion

### 4.1. Structures of the ATP complex and the AMPPXP complexes are slightly different

This work studied structural differences between the ATPase complexes with ATP, AMPPNP and AMPPCP. We confirm and substantiate a previous observation [40] that binding of ATP and of the ATP analog AMPPNP gives slightly different infrared difference spectra in the amide I spectral region which is sensitive to backbone structure and hydrogen bonding to the backbone carbonyl oxygens. In the case of AMPPCP, these differences could be recorded here with uprecedented accuracy because we were able to observe them directly in a time-resolved displacement experiment. The obtained nucleotide exchange spectrum (Fig. 2A, bold line) gives evidence that also the AMPPCP complex adopts a structure that is slightly different from that of the ATP complex, the difference being more pronounced at high $Ca^{2+}$ than at low $Ca^{2+}$/high $Mg^{2+}$. In contrast, the phosphorylation reaction $Ca_2$E1ATP → $Ca_2$E1P generates similar spectra in the presence and the absence of AMPPCP. This indicates that the structural change upon phosphorylation ($Ca_2$E1ATP → $Ca_2$E1P) is not affected by the presence of AMPPCP.

### 4.2. Difference in secondary structure between ATP and AMPPCP complex

The amplitude of the signals in the nucleotide exchange spectra is small but comparable to those of the phosphorylation reaction if the full extent of the AMPPCP → ATP exchange reaction is considered. For the phosphorylation spectrum in the absence of AMPPCP, the number of amide groups involved in a net secondary structure change has been estimated to be 3–10 [5] and we conclude that a similar number of residues is involved in the AMPPCP → ATP exchange reaction. These numbers seem to be realistic, as discussed previously [37], but it has to be kept in mind that they reflect the net change in secondary structure. The actual number of residues changing their structure can be considerably larger.

### 4.3. Molecular model of the structural differences between AMPPCP and ATP complex

The AMPPCP → ATP exchange spectra at high $Ca^{2+}$ (Fig. 2A and B) indicate that a β-sheet and a turn structure are involved in the structural difference between ATP and AMPPCP complex. The β-sheet is possibly the β-sheet in the P domain which interacts with the γ-phosphate and the ribose hydroxyls and changes structure upon nucleotide binding [11]. Since the presence of γ-phosphate and ribose hydroxyls has a drastic effect on the spectral change in the amide I region upon binding [6,7], a small displacement of them can explain the spectral differences between the ATPase complex with ATP and ATP analogs. Of these functional groups we suggest the γ-phosphate to cause the structural difference between ATP and AMPPXP complexes because the nucleotide exchange spectra are sensitive to the catalytic ion $Mg^{2+}$ or $Ca^{2+}$ that binds with the γ-phosphate. A shift of 0.3 Å of the γ-phosphate location can be expected from the different bond lengths and bond angles between β- and γ-phosphate of ATP and AMPPCP [41] (assuming no change in atomic positions for the rest of the nucleotide).

The different properties of the AMPPCP complex at high $Ca^{2+}$ and low $Ca^{2+}$/high $Mg^{2+}$, observed here and previously [16], may be explained by differences in ion coordination [16] at a crucial position between the two parts of the β-sheet in the P domain. With $Mg^{2+}$, the β-sheet seems to adopt very similar structures with ATP and AMPPCP as indicated by the small amplitude of bands in the β-sheet region of the nucleotide exchange spectrum (Fig. 2C). With $Ca^{2+}$, the structures are different. Changes in β-sheet structure could be transmitted further to the $Ca^{2+}$ binding sites for example via M4 which connects to one end of the β-sheet and contains the $Ca^{2+}$ gate [11,42,43] E309 or via interaction with the loop between transmembrane helices 6 and 7 of which helix 6 contains D800, a residue that coordinates both $Ca^{2+}$. Interestingly, the chromium complex of ATP leads to a stable $Ca^{2+}$ occluded complex [44,45].

### 4.4. The backbone structure of the AMPPCP complex is less "$Ca_2$E1P-like" than the ATP complex according to infrared spectroscopy

Because the AMPPCP complex at 10 mM $Ca^{2+}$ behaves in many respects like a $Ca_2$E1P analog [16] it could be expected that the AMPPCP complex is more "$Ca_2$E1P-like" than the ATP complex. In contrast to this expectation, the infrared spectrum of the AMPPCP complex at high $Ca^{2+}$ is less $Ca_2$E1P-like than that of the ATP complex. This holds for the amide I region which is sensitive to backbone structure and is true under both conditions tested, at high $Ca^{2+}$ and low $Ca^{2+}$/high $Mg^{2+}$, as discussed in the following. The relevant spectra are compared in Fig. 4 for the high $Ca^{2+}$ condition and we will consider four scenarios in the following.

(I) It can be assumed that the AMPPCP complex has the same structure as $Ca_2$E1P. In this case the AMPPCP→E1P spectrum (thin line) should not show any absorbance changes in the amide I region because the structures of AMPPCP complex and $Ca_2$E1P are the same. This is not observed, the AMPPCP→E1P spectrum exhibits signals in the amide I region which indicate that the structures of the AMPPCP complex and $Ca_2$E1P are different.

(II) The structure of the AMPPCP complex could resemble that of a transition state between the ATP complex and $Ca_2$E1P. We will discuss this scenario using marker bands for the $Ca_2$E1P structure. These are the positive bands in the phosphorylation spectrum without AMPPCP (dotted line) and in the AMPPCP→E1P spectrum (thin line), found at 1653 and 1637 $cm^{-1}$. In scenario II, the structure of the AMPPCP complex is closer to that of $Ca_2$E1P than the structure of the ATP complex. Thus, upon AMPPCP→ATP exchange, structural characteristics of $Ca_2$E1P should be lost and one should observe the $Ca_2$E1P bands as negative bands at 1653 and 1637 $cm^{-1}$ in the AMPPCP→ATP exchange spectrum. This is neither observed at high $Ca^{2+}$ (bold line in Fig. 4) nor at low $Ca^{2+}$/high $Mg^{2+}$ (bold line in Fig. 2C).

(III) It can be assumed that the structures of the ATP and the AMPPCP complex are identical. In this case, the AMPPCP→E1P spectrum (thin line in Fig. 4) should be identical to the phosphorylation spectrum in the absence of AMPPCP (reflecting $Ca_2$E1ATP→$Ca_2$E1P, dotted line). In addition, there should be no absorbance changes upon AMPPCP→ATP exchange (bold line spectrum). Both predictions of this scenario are not observed, indicating that the AMPPCP complex has a structure that is different from that of the ATP complex.

(IV) In the last scenario it will be assumed that the structure of the AMPPCP complex differs more from the $Ca_2$E1P structure than the ATP complex. In consequence, larger or additional conformational changes are required in the transition from the AMPPCP complex to $Ca_2$E1P than in the transition from the ATP complex. This will produce larger or additional bands for the former transition (thin line) than for the latter (dotted line). Clearly, this scenario describes our spectra best. The amplitudes of bands characteristic of $Ca_2$E1P (at 1653 and 1637 $cm^{-1}$) are larger for the transition from the AMPPCP complex and there is an additional negative band at 1673 $cm^{-1}$, not observed for the transition from the ATP complex. This negative band therefore indicates a structural characteristic of the AMPPCP complex that is neither present in the ATP complex, nor in $Ca_2$E1P. The same is true at low $Ca^{2+}$/high $Mg^{2+}$(bold line in Fig. 2C).

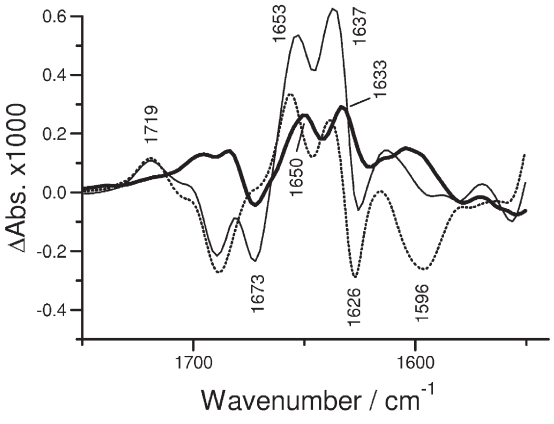


Fig. 4. Comparison of AMPPCP→ATP exchange spectrum (bold line), AMPPCP→E1P spectrum (thin line) and phosphorylation spectrum in the absence of AMPPCP (dotted line) at high $Ca^{2+}$. The latter spectrum was multiplied by 0.77 in order to normalize the spectra to the same amplitude at 1719 $cm^{-1}$ which is a marker band of the phosphorylation reaction. The larger amplitude of this band in the experiments without AMPPCP indicates higher accumulation of $Ca_2$E1P under these conditions or imperfections of the normalization to equal protein content.

Concluding this section on the backbone structure of the AMPPCP and ATP complexes, the spectral differences in the amide I region between nucleotide complex and $Ca_2$E1P are not smaller for AMPPCP than for ATP as could be expected from the results by Picard et al. Instead they are larger, indicating that also the structural differences are larger. This is based on the properties of bands throughout the amide I region, in particular the $Ca_2$E1P marker bands at 1653 and 1637 $cm^{-1}$ and the band at 1673 $cm^{-1}$ which is characteristic of the AMPPCP complex. The $Ca_2$E1P marker bands are not observed as negative bands in the AMPPCP→ATP exchange spectrum indicating that there is no loss of $Ca_2$E1P characteristics upon AMPPCP→ATP exchange. The negative 1673 $cm^{-1}$ band is only observed for AMPPCP indicating that additional structural changes are required in the transition from the AMPPCP complex to $Ca_2$E1P as compared to the transition from the ATP complex.

On the other hand, outside the amide I region there is a band at 1596 $cm^{-1}$ in the phosphorylation spectrum without AMPPCP (dotted line in Fig. 4) that is not present in the AMPPCP→E1P spectrum at high $Ca^{2+}$ (thin line) and at low $Ca^{2+}$/high $Mg^{2+}$ (thin line in Fig. 2C). Thus in this respect, the $Ca_2$E1AMPPCP complex is more like $Ca_2$E1P than like $Ca_2$E1ATP. The 1596 $cm^{-1}$ band is in the spectral region of the antisymmetric stretching vibration of carboxylate groups. It

does not shift in $^2H_2O$ [23] which indicates that the respective group is not in contact with water. In line with this, the rather high wavenumber indicates involvement in a salt bridge or ion chelation in a unidentate binding mode [31–33] if the tentative assignment to a carboxyl group is correct.

In conclusion, the infrared spectra indicate that the backbone structure of $Ca_2$E1AMPPCP is more distant from that of $Ca_2$E1P than that of $Ca_2$E1ATP. On the other hand a side chain interaction – possibly an ion chelating Asp or Glu residue – of $Ca_2$E1AMPPCP is like that in $Ca_2$E1P. The larger similarity in a side chain interaction of the AMPCP complex with $Ca_2$E1P cannot explain the $Ca_2$E1P-like properties of the AMPPCP complex at high $Ca^{2+}$ concentrations observed by Picard et al. [16] because it is also observed at low $Ca^{2+}$/high $Mg^{2+}$. The same two observations were made for AMPPNP at high $Ca^{2+}$ (not shown).

Thus it remains an apparent discrepancy between the expectation of a more $Ca_2$E1P-like structure of the AMPPCP complex at high $Ca^{2+}$ and the less $Ca_2$E1P-like backbone structure deduced from the infrared spectra at high $Ca^{2+}$ and low $Ca^{2+}$/high $Mg^{2+}$ as compared to the ATP complex. Possible explanations are:

(i) The ATPase could adopt a structure in the AMPPCP complex at high $Ca^{2+}$ which is different from that of $Ca_2$E1P and its ADP·$AlF_x$ analog but in spite of that behaves similarly regarding the properties probed by Picard et al. [16]. Thus there could be several structural ways for the ATPase to achieve similar functional properties.

(ii) The bands discussed might not be relevant for the observed functional properties or infrared spectroscopy might not observe the relevant structural changes. Infrared spectroscopy of the $Ca^{2+}$–ATPase seems to report predominantly conformational changes in well defined and stable backbone stretches, not of flexible hinge regions [6]. In line with this consideration, movement of the A domain towards the P domain does not contribute to a large extent to our spectra [6].

(iii) Protein concentration could be important. It is high, but comparable to physiological values in our infrared experiments and also high in crystals but much lower in the work by Picard et al. [16].

### *4.5. All ATPase nucleotide complexes studied here seem to adopt a closed conformation of the N and P domains*

In their interpretation of the different properties of the AMPPCP complex at high and low $Ca^{2+}$, Picard et al. [16] suggest that the ATPase nucleotide complexes could exist in different forms with bent and extended conformations of the nucleotide. The bent conformation would be adopted in solution at low $Ca^{2+}$ and would provide only little stabilization for the closed conformation of the cytoplasmic domains and allow $Ca^{2+}$ dissociation. The extended conformation, found in the crystals and with AMPPCP at high $Ca^{2+}$, would stabilize the closed conformation which occludes $Ca^{2+}$.

Reaction rates of ATPase phosphorylation [46], changes in fluorescence levels [47,48], and our infrared spectra [5,23] support the view that there is a conformational change in the reaction from the ATPase nucleotide complex to $Ca_2$E1P. It follows that the structures of the complex and that of the phosphoenzyme $Ca_2$E1P are different in line with the above suggestion.

At variance with the suggestion of an open conformation of the nucleotide–ATPase complex in solution however, our results indicate that all nucleotide ATPase complexes adopt a closed conformation at least for the N and P domains as discussed in the following first for ATP at high $Ca^{2+}$, then for AMPPNP at high $Ca^{2+}$ and finally for AMPPCP at high and low $Ca^{2+}$.

The spectral changes upon ATP binding are considerably larger than upon phosphorylation at high $Ca^{2+}$ [5] and at low $Ca^{2+}$/high $Mg^{2+}$ (not shown) indicating that most of the conformational change to the closed conformation takes place upon binding. Under our standard conditions of 10 mM $Ca^{2+}$, the nucleotide binding spectra are very sensitive to the presence of the ribose hydroxyls [6] and of the γ-phosphate [7], which is readily explained [37] by their interactions with the P domain in the closed conformation [11,12].

AMPPNP binding at 10 mM $Ca^{2+}$ causes very similar spectral changes (band positions and band amplitudes) as ATP binding [6,40], indicating that the interactions between ATPase and γ-phosphate as well as ribose hydroxyls of AMPPNP are largely in place. For this, γ-phosphate and ribose hydroxyls need to interact with the P domain in a closed structure of the AMPPNP complex.

AMPPCP at high $Ca^{2+}$ and low $Ca^{2+}$/high $Mg^{2+}$ behaves similarly to AMPPNP at 10 mM $Ca^{2+}$ as indicated by the similar AMPPXP→E1P spectra. This gives evidence for a closed structure also of the AMPPCP complexes irrespective of the $Ca^{2+}$ concentration. If a more open conformation were adopted in the ATPase AMPPCP complex under one of these conditions, bands characteristic of the transition into the closed conformation [6] should be observed in AMPPCP→E1P spectra, in particular the ATP binding bands at 1641 and 1627 $cm^{-1}$ [5,6,40]. They have a much larger amplitude ($\Delta\Delta A_{1627-1641}$ = 0.0035) than bands in the AMPPCP→E1P spectra (max $\Delta A$ = 0.0002), transition into the closed conformation should therefore easily be detected. However, the bands are not observed in the AMPPCP→E1P spectra at high and low $Ca^{2+}$, confirming that the AMPPCP complex adopts a closed conformation under both conditions. For a different nucleotide – ITP – on the other hand, these bands have been observed in the phosphorylation reaction with ITP [37]. ITP causes only a small conformational change upon binding [6] indicating a more open conformation of the ATPase ITP complex and requiring part of the transition to the closed conformation to be performed in the subsequent phosphorylation reaction.

## 5. Conclusions

The structure of the ATPase complex with ATP is only slightly different from those with AMPPCP and AMPPNP and

all complexes seem to form a closed conformation. The structure of one or several turns is more $Ca_2E1P$-like in the complex with ATP than in the complexes with the ATP analogs AMPPCP and AMPPNP. The structure of a β-sheet, likely the β-sheet in the P domain, is similar for the AMPPCP and ATP complexes with $Mg^{2+}$ as catalytic ion, but different with $Ca^{2+}$. This is likely caused by differences in ion coordination that affect the structure of the β-sheet in the P domain and which are further transmitted to the $Ca^{2+}$ binding sites where they affect $Ca^{2+}$ dissociation as observed previously [16].

## Acknowledgements

We are grateful to W. Hasselbach (Max-Planck-Institut, Heidelberg) for the gift of $Ca^{2+}$–ATPase, to J. E. T. Corrie (National Institute for Medical Research, London) and to F. von Germar for the preparation of caged compounds.

## References

[1] W. Hasselbach, M. Makinose, Die Calciumpumpe der "Erschlaffungsgrana" des Muskels und ihre Abhängigkeit von der ATP-Spaltung, Biochem. Z. 333 (1961) 518–528.
[2] J.P. Andersen, Monomer–oligomer equilibrium of sarcoplasmic reticulum Ca-ATPase and the role of subunit interaction in the $Ca^{2+}$ pump mechanism, Biochim. Biophys. Acta 988 (1989) 47–72.
[3] E. Mintz, F. Guillain, $Ca^{2+}$ transport by the sarcoplasmic reticulum ATPase, Biochim. Biophys. Acta 1318 (1997) 52–70.
[4] W. Hasselbach, The sarcoplasmic calcium pump, Top. Curr. Chem. 78 (1979) 1–56.
[5] A. Barth, F. von Germar, W. Kreutz, W. Mäntele, Time-resolved infrared spectroscopy of the $Ca^{2+}$–ATPase. The enzyme at work, J. Biol. Chem. 271 (1996) 30637–30646.
[6] M. Liu, A. Barth, Mapping interactions between the $Ca^{2+}$–ATPase and its substrate ATP with infrared spectroscopy, J. Biol. Chem. 278 (2003) 10112–10118.
[7] M. Liu, A. Barth, Mapping nucleotide binding site of calcium ATPase with IR spectroscopy: effects of ATP_-phosphate binding, Biopolymers (Biospectroscopy) 67 (2002) 267–270.
[8] M. Liu, A. Barth, TNP-AMP binding to the sarcoplasmic reticulum $Ca^{2+}$–ATPase studied by infrared spectroscopy, Biophys. J. 85 (2003) 3262–3270.
[9] D.L. Stokes, N.M. Green, Modeling a dehalogenase fold into the 8-Å density map for $Ca^{2+}$–ATPase defines a new domain structure, Biophys. J. 78 (2000) 1765–1776.
[10] D.B. McIntosh, The ATP binding sites of P-type ion transport ATPase: properties, structure, conformations, and mechanism of energy coupling, Adv. Mol. Cell Biol. 23A (1998) 33–99.
[11] C. Toyoshima, T. Mizutani, Crystal structure of the calcium pump with a bound ATP analogue, Nature 430 (2004) 529–535.
[12] T.L.-M. Sørensen, J.V. Møller, P. Nissen, Phosphoryl transfer and calcium ion occlusion in the calcium pump, Science 304 (2004) 1672–1675.
[13] D.L. Stokes, N.M. Green, Structure and function of the calcium pump, Annu. Rev. Biophys. Biomol. Struct. 32 (2003) 445–468.
[14] C. Toyoshima, G. Inesi, Structural basis of ion pumping by $Ca^{2+}$–ATPase of the sarcoplasmic reticulum, Annu. Rev. Biochem. 73 (2004) 269–292.
[15] C. Toyoshima, H. Nomura, T. Tsuda, Lumenal gating mechanism revealed in calcium pump crystal structures with phosphate analogues, Nature 432 (2004) 361–368.
[16] M. Picard, C. Toyoshima, P. Champeil, The average conformation at micromolar [$Ca^{2+}$] of $Ca^{2+}$–ATPase with bound nucleotide *differs* from that adopted with the transition state analog ADP·$AlF_x$ or with AMPPCP under crystallization conditions at millimolar [$Ca^{2+}$], J. Biol. Chem. 280 (2005) 18745–18754.
[17] A. Barth, C. Zscherp, Substrate binding and enzyme function investigated by infrared spectroscopy, FEBS Lett. 477 (2000) 151–156.
[18] A. Barth, Time-resolved IR spectroscopy with caged compounds: an introduction, in: M. Goeldner, R.S. Givens (Eds.), Dynamic Studies in Biology: Phototriggers, Photoswitches and Caged Biomolecules, Wiley-VCH, Weinheim, 2005.
[19] V. Jayaraman, IR spectroscopy with caged compounds: selected applications, in: M. Goelder, R.S. Givens (Eds.), Dynamic Studies in Biology: Phototriggers, Photoswitches and Caged Biomolecules, Wiley-VCH, Weinheim, 2005.
[20] A. Barth, Selective monitoring of 3 out of 50,000 protein vibrations, Biopolymers (Biospectroscopy) 67 (2002) 237–241.
[21] A. Barth, W. Mäntele, W. Kreutz, Infrared spectroscopic signals arising from ligand binding and conformational changes in the catalytic cycle of sarcoplasmic reticulum $Ca^{2+}$–ATPase, Biochim. Biophys. Acta 1057 (1991) 115–123.
[22] R.J. Ellis, Macromolecular crowding: an important but neglected aspect of the intracellular environment, Curr. Opin. Struct. Biol. 11 (2001) 114–119.
[23] A. Barth, W. Mäntele, ATP-induced phosphorylation of the sarcoplasmic reticulum $Ca^{2+}$ ATPase: molecular interpretation of infrared difference spectra, Biophys. J. 75 (1998) 538–544.
[24] A. Barth, W. Kreutz, W. Mäntele, Changes of protein structure, nucleotide microenvironment, and $Ca^{2+}$ binding states in the catalytic cycle of sarcoplasmic reticulum $Ca^{2+}$ ATPase: investigation of nucleotide binding, phosphorylation and phosphoenzyme conversion by FTIR difference spectroscopy, Biochim. Biophys. Acta 1194 (1994) 75–91.
[25] J. Andersson, A. Barth, FTIR studies on the bond properties of the aspartyl phosphate moiety of the $Ca^{2+}$–ATPase, Biopolymers 82 (2006) 353–357.
[26] A. Barth, W. Mäntele, W. Kreutz, Molecular changes in the sarcoplasmic reticulum $Ca^{2+}$ ATPase during catalytic activity. A Fourier transform infrared (FTIR) study using photolysis of caged ATP to trigger the reaction cycle, FEBS Lett. 277 (1990) 147–150.
[27] A. Barth, J.E.T. Corrie, M.J. Gradwell, Y. Maeda, W. Mäntele, T. Meier, D .R. Trentham, Time-resolved infrared spectroscopy of intermediates and products from photolysis of 1-(2-nitrophenyl)ethyl phosphates: reaction of the 2-nitrosoacetophenone byproduct with thiols, J. Am. Chem. Soc. 119 (1997) 4149–4159.
[28] E. Goormaghtigh, V. Cabiaux, J.-M. Ruysschaert, Determination of soluble and membrane protein structure by Fourier transform infrared spectroscopy. III. Secondary structures, Subcell. Biochem. 23 (1994) 405–450.
[29] M. Jackson, H.H. Mantsch, The use and misuse of FTIR spectroscopy in the determination of protein structure, Crit. Rev. Biochem. Mol. Biol. 30 (1995) 95–120.
[30] A. Barth, The infrared absorption of amino acid side chains, Prog. Biophys. Mol. Biol. 74 (2000) 141–173.
[31] J.E. Tackett, FT-IR characterisation of metal acetates in aqueous solution, Appl. Spectrosc. 43 (1989) 483–489.
[32] G.B. Deacon, R.J. Phillips, Relationships between the carbon-oxygen stretching frequencies of carboxylate complexes and the type of carboxylate coordination, Coord. Chem. Rev. 33 (1980) 227–250.
[33] M. Nara, H. Torii, M. Tasumi, Correlation between the vibrational frequencies of the carboxylate group and the types of its coordination to a metal ion: an ab initio molecular orbital study, J. Phys. Chem. 100 (1996) 19812–19817.
[34] S.W. Englander, N.R. Kallenbach, Hydrogen exchange and structural dynamics of proteins and nucleic acids, Q. Rev. Biophys. 4 (1984) 521–655.
[35] H.H.J. De Jongh, E. Goormaghtigh, J.-M. Ruysschaert, Monitoring structural stability of trypsin inhibitor at the submolecular level by amide–proton exchange using Fourier transform infrared spectroscopy: a test case for more general application, Biochemistry 36 (1997) 13593–13602.
[36] C. Vigano, M. Smeyers, V. Raussens, F. Scheirlinckx, J.M. Ruysschaert, E. Goormaghtigh, Hydrogen–deuterium exchange in membrane proteins monitored by IR spectroscopy: a new tool to resolve protein structure and dynamics, Biopolymers 74 (2004) 19–26.
[37] M. Liu, A. Barth, Phosphorylation of the sarcoplasmic reticulum $Ca^{2+}$–ATPase from ATP and ATP analogs studied by infrared spectroscopy, J. Biol. Chem. 279 (2004) 49902–49909.

[38] Y.N. Chirgadze, N.A. Nevskaya, Infrared spectra and resonance interaction of amide—I vibration of the antiparallel-chain pleated sheet, Biopolymers 15 (1976) 607–625.
[39] J. Kubelka, T.A. Keiderling, Differentiation of β-sheet-forming sturctures: ab initio-based simulations of IR absorption and vibrational CD for model peptide and protein β-sheets, J. Am. Chem. Soc. 123 (2001) 12048–12058.
[40] F. Von Germar, A. Barth, W. Mäntele, Structural changes of the sarcoplasmic reticulum $Ca^{2+}$–ATPase upon nucleotide binding studied by Fourier transform infrared spectroscopy, Biophys. J. 78 (2000) 1531–1540.
[41] R.G. Yount, D. Babcock, W. Ballatyne, D. Ojala, Adenylyl imidodiphosphate, an adenosine triphosphate analog containing a P–N–P linkage, Biochemistry 10 (1971) 2484–2489.
[42] B. Vilsen, J.P. Andersen, Mutation to the glutamate in the fourth membrane segment of $Na^+$,$K^+$–ATPase and $Ca^{2+}$–ATPase affects cation binding from both sides of the membrane and destabilizes the occluded enzyme forms, Biochemistry 37 (1998) 10961–10971.
[43] G. Inesi, H. Ma, D. Lewis, C. Xu, $Ca^{2+}$ occlusion and gating function of $Glu^{309}$ in the ADP-fluoroaluminate analog of the $Ca^{2+}$–ATPase phosphoenzyme intermediate, J. Biol. Chem. 279 (2004) 31629–31637.
[44] E.H. Serpersu, U. Kirch, W. Schoner, Demonstration of a stable occluded form of $Ca^{2+}$ by the use of the chromium complex of ATP in the $Ca^{2+}$–ATPase of sarcoplasmic reticulum, Eur. J. Biochem. 122 (1982) 347–354.
[45] B. Vilsen, J.P. Andersen, Occlusion of $Ca^{2+}$ in soluble monomeric sarcoplasmic reticulum $Ca^{2+}$–ATPase, Biochim. Biophys. Acta 855 (1986) 429–431.
[46] J.R. Petithory, W.P. Jencks, Phosphorylation of the calcium adenosinetriphosphatase of sarcoplasmic reticulum: rate-limiting conformational change followed by rapid phosphoryl transfer, Biochemistry 25 (1986) 4493–4497.
[47] H. Suzuki, S. Nakamura, T. Kanazawa, Effects of divalent cations bound to the catalytic site on ATP-induced conformational changes in the sarcoplasmic reticulum $Ca^{2+}$–ATPase: stopped-flow analysis of the fluorescence of *N*-acetyl-*N*′-(5-sulfo-1-naphthyl)ethylenediamine attached to cysteine-674, Biochemistry 33 (1994) 8240–8246.
[48] S. Nakamura, H. Suzuki, T. Kanazawa, The ATP-induced change of tryptophan fluorescence reflects a conformational change upon formation of ADP-sensitive phosphoenzyme in the sarcoplasmic reticulum $Ca^{2+}$–ATPase—stopped-flow spectrofluorometry and continuous-flow rapid quenching method, J. Biol. Chem. 269 (1994) 16015–16019.